Available online at www.sciencedirect.com

SciVerse ScienceDirect

Journal of Nutritional Biochemistry 24 (2013) 496–504

Journal of Nutritional Biochemistry

The flavonoids diosmetin and luteolin exert synergistic cytostatic effects in human hepatoma HepG2 cells via CYP1A-catalyzed metabolism, activation of JNK and ERK and P53/P21 up-regulation☆

Vasilis P. Androutsopoulos*, Demetrios A. Spandidos

Laboratory of Clinical Virology, University of Crete, Voutes, Heraklion, 71409, Crete, Greece

Received 26 August 2011; received in revised form 22 December 2011; accepted 31 January 2012

Abstract

Various types of tumors are known to overexpress enzymes belonging to the CYP1 family of cytochromes P450. The present study aimed to characterize the metabolism and further antiproliferative activity of the natural flavonoid diosmetin in the CYP1-expressing human hepatoma cell line HepG2. Diosmetin was converted to luteolin in HepG2 cells after 12 and 30 h of incubation. In the presence of the CYP1A inhibitor α-naphthoflavone, the conversion of diosmetin to luteolin was attenuated. 3-(4,5-Dimethylthiazol-2-yl)-2,5-diphenyltetrazolium bromide assays revealed luteolin to be more cytotoxic than diosmetin. The antiproliferative effect of diosmetin in HepG2 cells was attributed to blockage at the G2/M phase as determined by flow cytometry. Induction of G2/M arrest was accompanied by up-regulation of phospho-extracellular-signal-regulated kinase (p-ERK), phospho-c-jun N-terminal kinase, p53 and p21 proteins. More importantly, induction of G2/M arrest and p53 and p-ERK up-regulation were reversed by the application of the CYP1 inhibitor α-naphthoflavone. Taken together, the data provide new evidence on the tumor-suppressing role of cytochrome P450 CYP1A enzymes and extend the hypothesis that the anticancer activity of dietary flavonoids is enhanced by P450-activation.

Keywords: Flavonoids; Diosmetin; Luteolin; Cytochrome P450 CYP1 enzymes; Antiproliferation; Liver cancer

1. Introduction

Hepatocellular carcinoma is the fourth leading cause of cancer death worldwide [1]. The 5-year survival rate for this disease is estimated at 7%. Treatment options for liver cancer mainly focus on chemotherapy, e.g., the alkylating agent cisplatin or the topoisomerase inhibitor doxorubicin [1,2]. Although the use of these chemotherapeutic regimens is well established, the major drawback encountered is their limited specificity for the tumor site. Hence, in the past two decades, considerable effort has been made to develop new drugs with enhanced specificity and improved efficacy towards liver cancer. Natural products have played a pivotal role in the quest for developing novel chemotherapeutic agents with enhanced specificity and potency. Some examples include semisynthetic derivatives of taxanes or the flavone derivative flavopiridol [3,4].

Diosmetin is a flavone found in various dietary sources, such as oregano spice, oregano leaves, citrus fruits and extracts from specific medicinal herbs, such as *Rosa agrestis* Savi (Rosaceae), *Chrysanthemum morifolium* (Asteraceae), *Anastatica hierochuntica* L. (Brassicaceae) and *Dianthus versicolor* Fisch (Caryophyllaceae) [5–10]. The latter plant contains a mixture of flavonoids and is used in traditional Mongolian medicine against liver diseases [11]. Luteolin is structurally related to diosmetin; instead of a methoxy group at the 4′ position of the B ring, this compound contains a hydroxyl group. Luteolin is found in various common dietary sources, notably artichoke, chamomile and olive oil [12–14]. Luteolin has demonstrated anticancer activity in cancer cell lines and *in vivo* models [15]. This type of activity has been attributed to activation of apoptosis, cell cycle arrest and inhibition of tumor invasion [15].

In a recent study, we demonstrated that diosmetin is converted to luteolin by recombinant cytochrome P450 CYP1A1, CYP1B1 and CYP1A2, as well as in breast adenocarcinoma cells that express CYP1 enzymes [16]. The latter enzymes have been implicated in carcinogenesis, and their elevated expression in tumor cells has made them plausible targets for novel chemotherapeutic drugs [17]. Extrahepatic CYPs, notably CYP1B1 and CYP1A1, may be utilized to target tumor cells by the use of selective antibodies or the activation of prodrugs that are inactive in tissues or cells that do not express these enzymes [18,19]. Our previous reports suggest that several flavonoids including diosmetin are substrates for CYP1 enzymes and possess therapeutic implications if their conversion products can inhibit tumor cell growth [20].

Abbreviations: CYP1A, cytochrome P450 CYP1A1 and CYP1A2; HPLC, high pressure liquid chromatography; IC50, 50% inhibitory concentration; MTT, 3-(4,5-dimethylthiazol-2-yl)-2,5-diphenyltetrazolium bromide; ERK, extracellular-signal-regulated kinase; JNK, c-jun N-terminal kinase.

☆ Conflict of interest: none declared.

* Corresponding author. Tel.: +30 2810 394633.

E-mail address: vandrou@med.uoc.gr (V.P. Androutsopoulos).

0955-2863/$ - see front matter © 2013 Elsevier Inc. All rights reserved.
http://dx.doi.org/10.1016/j.jnutbio.2012.01.012

In order to address whether CYP1 metabolism of diosmetin mediates an antiproliferative effect in cancer types other than breast, we used the human hepatoma cell line HepG2 that expresses CYP1 enzymes to investigate the metabolism of diosmetin and determine the antiproliferative activity of this flavone and its putative metabolic product luteolin *in vitro*.

2. Materials and methods

2.1. Chemicals and antibodies

3-(4,5-Dimethylthiazol-2-yl)-2,5-diphenyltetrazolium bromide (MTT), propidium iodide (PI), α-naphthoflavone, tissue culture reagents and media, Western blotting lysis buffer and dithiothreitol (DTT) were purchased from Sigma Aldrich (Life Science Chemicals, Athens, Greece). Diosmetin was purchased from Extrasynthese (Lyon, France), and luteolin was from Lab-supplies (Athens, Greece). Western blotting reagents were from Bio-Rad (Athens, Greece), whereas reverse transcriptase polymerase chain reaction (PCR) reagents were from Lab-supplies (Athens, Greece). Polyclonal antibodies against nuclear factor kappa B (NF-kB) and phospho-extracellular-signal-regulated kinase (p-ERK) and monoclonal antibodies against p53 and p21 were from Santa Cruz Biotechnology (Heidelberg, Germany). Polyclonal antibodies against c-jun N-terminal kinase (JNK) and phospho-JNK (p-JNK) were from Upstate Cell signaling, UK. Monoclonal antibody against β-actin was from Sigma-Aldrich (Life Science Chemicals, Athens, Greece). Secondary antibodies for Western blotting were from Santa Cruz Biotechnology.

2.2. Cell culture

HepG2 cells were maintained in Dulbecco's modified Eagle's medium (DMEM) with glutamine containing 10% heat-inactivated fetal bovine serum (FBS) and penicillin/streptomycin ×1. The cells were grown in a humidified incubator at 37°C in 5% CO_2/95% air and passaged using trypsin EDTA (0.25% v/v) every 3 to 4 days.

2.3. 7-Ethoxyresorufin-O-deethylase (EROD) assay

EROD activity was measured in HepG2 cells as described previously [21]. Briefly, cells were grown in 96-well plates prior to the experiment. The cells were washed twice with phosphate-buffered saline (PBS), and 7-ethoxyresorufin was added in DMEM at a final concentration of 5 μM in the presence of salicylamide (1.5 mM). The cells were incubated with 7-ethoxyresorufin for 1 h, and aliquots from media were transferred into Eppendorf vials. The reaction was quenched with equal volumes of ice-cold methanol. The samples were centrifuged for 10 min at 4000 rpm, and fluorescence was measured in a microplate fluorescence reader (FL_X800 Biotech Instruments, Winooski, VT, USA) with λexc of 530 nm and λemi at 590 nm.

2.4. RNA extraction and real-time PCR

HepG2 cells were grown in T75 flasks, and total RNA was extracted using Trizol. Briefly, 1 ml of Trizol reagent was added to each flask, and the resulting sample was mixed with 200 μl of chloroform and centrifuged at 14,000 rpm for 15 min at 4°C. RNA was removed from the top layer, mixed with an equal volume of ice-cold isopropanol and centrifuged at 13,000 rpm for 5 min. The resulting pellet containing the RNA was precipitated with 70% ice-cold ethanol and further centrifuged at 7500 rpm for 10 min. The RNA pellet was dissolved in 25 μl of sterile H_2O. Total RNA was checked for purity by spectrophotometry. RNA was treated with DNase for 45 min at 43°C in order to avoid any possible contamination. cDNA was synthesized using a Promega kit according to the manufacturer's instructions. Real-time PCR was performed with an M_X3000 Stratagene PCR amplifier using 20 μl as the total volume of each reaction. Ten microliters of SYBR Green master mix was mixed with 1.2 μl of forward and reverse primer and 0.5 μl of unknown cDNA and 8.3 μl of H_2O. The annealing temperature was 60°C for all four sets of primers. Primer sequences for CYP1A1, CYP1B1 and CYP1A2 were obtained from previously published data [22]. Forty cycles were used for each gene amplification.

2.5. Flavonoid metabolism in HepG2 cells

HepG2 cells were seeded in T25 flasks at a density of $2x10^4$ cells/ml and cultured for 48 h at 37°C. Diosmetin was added to the media, and samples were obtained at the time points 0, 12 and 30 h. An initial stock concentration was made at 10 mM in dimethyl sulfoxide (DMSO) and then diluted with DMEM. Diosmetin was added at a concentration of 30 μM or 50 μM. The reaction was terminated by addition of an equal volume of methanol:acetic acid (100:1 v/v). Incubates were centrifuged at 13,000 rpm for 20 min at 4°C, and supernatants were analyzed by reversed-phase high-performance liquid chromatography (HPLC).

2.6. Flavonoid metabolism by recombinant CYPs

Incubations were performed in the presence of diosmetin, $MgCl_2$, phosphate buffer and NADPH as described previously [16]. Recombinant CYP2 and CYP3 enzymes were added to give a final concentration of 20 pmol/ml. The reaction was terminated after 20 min by addition of equal volumes of methanol:acetic acid (100:1 v/v). Samples were centrifuged for 20 min at 4°C at 13,000 rpm, and the supernatants were analyzed by HPLC.

2.7. HPLC analysis

The method has been described in detail in previous publications [16]. Briefly, a Luna C18 4.6×150-mm 5-μ column was used with a mobile phase containing solvents A and B. Solvent A contained 1% acetonitrile and 0.5% acetic acid in H_2O, and solvent B contained 4% acetonitrile and 0.5% acetic acid in MeOH. The following gradient was used: 60% solvent A and 40% solvent B at time=0 min and 10% solvent A and 90% solvent B at time=10 min. Final conditions were maintained for 1 min prior to returning to the initial solvent conditions with 8 min remaining for column equilibration after each run. Detection of diosmetin–luteolin was monitored using a Waters Series 200 UV detector (Waters, Hertfordshire, UK) at 360 nm. The concentrations of diosmetin and luteolin were determined using a calibration curve covering the concentration range of 0.5–50 and 0.2–20 μM for each compound, respectively. The analyses were carried out at 37°C at a flow rate of 1 ml/min. Average recovery for diosmetin and luteolin was estimated to be 85%.

2.8. MTT assay

HepG2 cells ($1×10^4$ cells/ml) were seeded in 96-well plates, and the antiproliferative effects of diosmetin and luteolin were assayed as described previously [21]. Inhibition experiments were performed in the presence of 0.5-1 μM α-naphthoflavone.

2.9. Isobologram analysis

Isobologram plots were generated by estimating the concentrations responsible for 10%, 20%, 30%, 40%, 50%, 60% and 70% inhibition of cellular proliferation for diosmetin in the presence of the CYP1A inhibitor α-naphthoflavone (0.5 μM) alone, luteolin alone and diosmetin in the presence of α-naphthoflavone with luteolin. The concentration points of diosmetin (+I) alone were plotted in the *x*-axis, whereas the concentration points for luteolin alone plotted in the *y*-axis. The concentration points for the combined action of the two compounds were plotted as an *XY* scatter. Additive lines were plotted for each percentage of inhibition (10%–70%) connecting the concentration points of each compound alone.

2.10. Fluorescence-activated cell sorting analysis

HepG2 cells were cultured in T75 flasks. Cells were incubated for 24 h in the presence of diosmetin (20 or 40 μM), with or without the addition of α-naphthoflavone. The cells were washed once with PBS, trypsinized and collected in a sterile Eppendorf vial. The cellular pellet was fixed in 70% ethanol for at least 2 h. PI was added to the cellular pellet at a final concentration of 50 μg/ml with RNase A (100 μg/ml). Fluorescence intensity was measured using a Beckman Coulter flow cytometer at PMT4. At least 10,000 events were acquired. Data analysis and acquisition were performed as described in previous publications [21].

2.11. Western blotting

HepG2 cells were cultured in T25 flasks to a density of $5×10^5$ cells/ml and incubated at 37°C for 24 h in the presence of diosmetin or luteolin (0, 30, 50, 70 μM). Following medium withdrawal, the cells were lysed with 100 μl of lysis buffer containing protease inhibitor cocktail and DL-DTT (1 mM), sonicated on ice for 5 min and finally centrifuged at 13,000 rpm at 4°C for 15 min. The protein concentration required for the experiment was adjusted to 0.7 mg/ml for each sample, and the protein lysate was mixed with sample buffer at a 1:1 ratio. Samples were heated at 100°C for 5 min and then loaded on an acrylamide gel. Electrophoresis was carried out for 1 h at 120 V/cm, and the proteins were transferred by wet blotting to a polyvinylidene fluoride membrane. The membrane was incubated in 10% milk/0.05% TBST (Tris-Borate/Tween 20) at room temperature for 1 h by continuous shaking. Incubation with NF-kB, p-ERK, JNK and p-JNK primary antibodies was performed in 1% milk/0.05% TBST at 4°C overnight. Antibody dilutions used were 1:400, 1:200, 1:400 and 1:400, respectively. Incubation for p53, p21 and β-actin proteins was performed for 2 h at room temperature in 1% milk/0.05% TBST at 1:500 dilutions. Each membrane was subsequently washed three times with 0.05% TBST and incubated with the secondary antibody against horseradish peroxidase diluted in 1% milk/0.05% TBST at room temperature for 1.5 h. The membranes were finally exposed to ECL reagents, and the electrophoretograms were developed on film.

2.12. Statistical analysis

Data are presented as the mean of at least three independent measurements and were analyzed by the paired *t* test and one-way analysis of variance with Dunnet's posttest as indicated using GraphPad Prism. Error bars represent mean±S.D. for at least $n=3$ determinations.

3. Results

3.1. CYP1 expression in HepG2 cells

Previous studies have demonstrated that HepG2 cells express CYP1A1 and, to a lesser extent, CYP1A2/CYP1B1 [22,23]. In order to confirm this finding, human hepatoma HepG2 cells were incubated with 7-ethoxyresorufin for 45 min to test the activity levels of CYP1 enzymes. EROD activity is notably indicative of CYP1A expression, as demonstrated by previous studies [24]. Samples taken from HepG2 cellular extracts showed approximately 2- to 2.5- fold higher fluorescence compared to samples from medium extracts that contained no cells (Fig. 1A). To further explore which of the three CYP1-enzymes was expressed to a higher extent, quantitative PCR (qPCR) was used to quantify the mRNA expression levels of CYP1A2, CYP1A1 and CYP1B1. CYP1A1 was expressed at the highest levels, followed by CYP1A2 and CYP1B1 (Fig. 1B). The mRNA expression levels of CYP1B1 were very low and almost undetectable, indicating that CYP1A enzymes are the main contributors of EROD activity in HepG2 cells.

3.2. Diosmetin is metabolized to luteolin in HepG2 cells

Diosmetin and luteolin were separated by reversed-phase HPLC. Diosmetin eluted at approximately 12.2 min, whereas luteolin eluted at approximately 11 min (Fig. 2A). Incubation of HepG2 cells with 30 μM of diosmetin yielded a metabolite that eluted at approximately 11 min (Fig. 2B). This metabolite was not detected at the start of the incubation (time=0 h) (Fig. 2B). Spiking of a HepG2 incubate with a small concentration of luteolin (0.4 μM) resulted in an increase in the total area of the metabolite, indicating that it coeluted with luteolin (Fig. 2B). This finding suggested that the metabolite present in the HepG2 cellular extract was luteolin.

3.3. Luteolin metabolism in HepG2 cells is CYP1A selective

In order to confirm that the metabolism of diosmetin to luteolin in HepG2 cells is CYP1A mediated, the parent compound was incubated for 12- and 30-h time points in the presence or absence of the CYP1A inhibitor α-naphthoflavone, and the metabolism was analyzed by HPLC. It must be emphasized that α-naphthoflavone inhibits mainly CYP1A1, and CYP1A2 to a lesser degree. In the absence of the inhibitor, the concentration of luteolin after a 12-h incubation was approximately 6.5 μM, whereas in the presence of inhibitor, the concentration of luteolin only reached approximately 1 μM (Figs. 2C and 3B). After 30 h of incubation without inhibitor, the concentration of luteolin had increased to approximately 10.5 μM (Fig. 2C). In the presence of α-naphthoflavone, the concentration of luteolin had not significantly increased further after 30-h incubation (Fig. 3A and B). The concentration of diosmetin ranged from 25 μM at 0 h to 22 and 15 μM in the presence and absence of the CYP1A inhibitor respectively at 12 h (Figs. 2C and 3B).

3.4. Diosmetin metabolism by a hepatic CYP panel

HepG2 cells do not fully reflect liver metabolism since several P450s are not expressed at sufficient levels in this cancer cell line [25,26]. In order to find out whether diosmetin is metabolized by hepatic CYPs, the compound was incubated with recombinant CYP enzymes that are usually expressed in the liver (CYP2A6, CYP2B6, CYP2C8, CYP2C9, CYP2C19, CYP2D6, CYP2E1, CYP3A5). The mixture was left to incubate for 20 min, and the lysate was analyzed by HPLC. The concentration of diosmetin fluctuated at the level of 10 μM, which was the initial starting concentration,

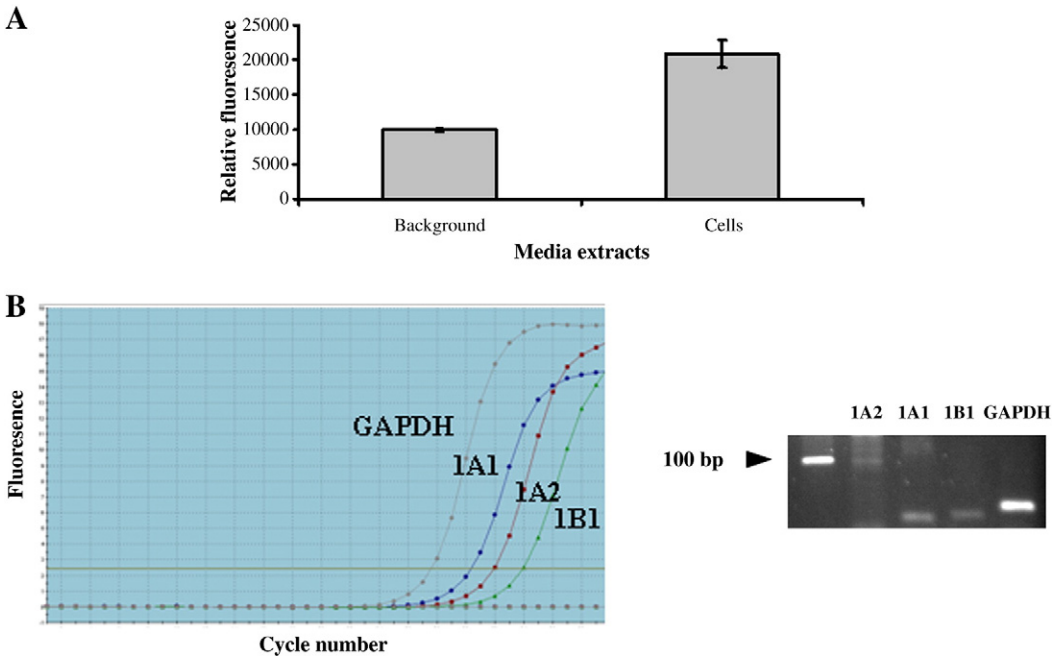

Fig. 1. Cytochrome P450 CYP1 expression in human hepatoma HepG2 cells. (A) HepG2 cells were cultured in 96-well plates, and EROD assay was carried out as described in Materials and Methods. Experiments were performed at least three times, and error bars indicate S.D. of the mean. (B) Real-time PCR amplification curves for CYP1A1, CYP1A2, CYP1B1 and GAPDH mRNA transcripts. RNA from HepG2 cells was extracted with Trizol, reverse transcribed and amplified as described in Materials and Methods.

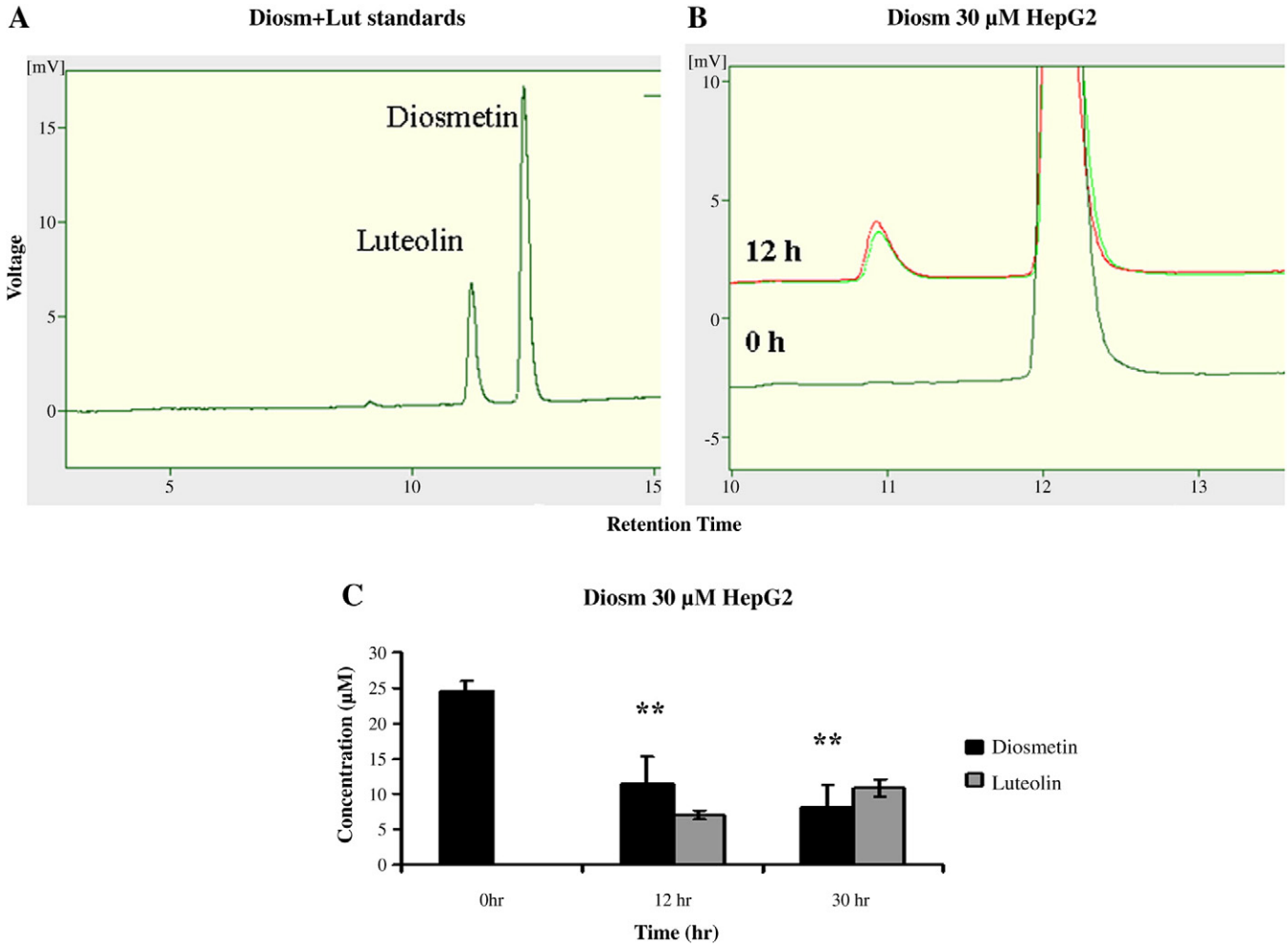

Fig. 2. HPLC analysis of diosmetin and luteolin in HepG2 cells. (A) Retention time of diosmetin and luetolin standards, as separated by the HPLC methodology used in the study. (B) Coelution profile of luteolin in HepG2 cells. Diosmetin (30 µM) was incubated with HepG2 cells for 0 and 12 h, and the samples were analyzed by HPLC. The 12-h incubate was spiked with a low concentration of luteolin (0.4 µM). (C) Concentrations of diosmetin and luteolin after incubation with HepG2 cells for 0, 12 and 30 h. Error bars indicate S.D. of the mean for $n=3$ determinations. **Statistically different compared to control ($P<.01$).

and did not show a significant decrease over the 20-min period (Fig. 4). HPLC analysis did not reveal any metabolites present (data not shown).

3.5. Diosmetin and luteolin inhibit proliferation of HepG2 cells

The potency of diosmetin and luteolin to inhibit proliferation of HepG2 cells was evaluated using the MTT assay. Diosmetin gave a 50% inhibitory concentration (IC50) of approximately 30 µM in the presence and absence of the CYP1A inhibitor α-naphthoflavone (Fig. 5A). This inhibitor was used at concentrations of 0.5–1 µM. Luteolin was more active than diosmetin, with an IC50 value of 15 µM in the presence and absence of the inhibitor α-naphthoflavone (Fig. 5B). In order to establish whether diosmetin and luteolin act synergistically in inhibiting proliferation of HepG2 cells, the two flavonoids were incubated simultaneously with HepG2 cells, and cell viability was assessed with the MTT assay as described above. The combined effect of the two compounds produced a markedly lower IC50 of approximately 7 µM compared to the IC50 noted with either compound alone (Fig. 5C). In addition, isobologram analysis was performed to elucidate whether the effect is additive or synergistic. The concentrations of compounds that were responsible for 10%–70% inhibition of cell proliferation were plotted at the *x*- and *y*-axis of the graph, whereas the data points assigned indicated the concentrations responsible for 10%–70% inhibition of cell proliferation of the combined treatment of diosmetin and luteolin (Fig. 5D). The results are indicative of a synergistic mode of action since the data points that correspond to the combined treatment of diosmetin and luteolin were below the additive line of the isobologram plot (Fig. 5D).

3.6. Diosmetin induces G2/M arrest in HepG2 cells

The cell cycle profile of HepG2 cells following treatment with diosmetin for 24 h was investigated using flow cytometry. A concentration of 20 µM diosmetin seemed to induce a short G1 phase arrest, although the results were not statistically significant (Fig. 6B). Significant S phase decrease and G2/M phase arrest (from 20% in control samples to 30% in diosmetin-treated samples) were seen after treatment of 20 µM of diosmetin (Fig. 6B). The results were similar in the presence of the CYP1A inhibitor α-naphthoflavone (Fig. 6B). However, when a higher concentration of diosmetin was used (40 µM), the arrest at G2/M phase was greater and partially reversible by coincubation with the CYP1A inhibitor (Fig. 6A and B).

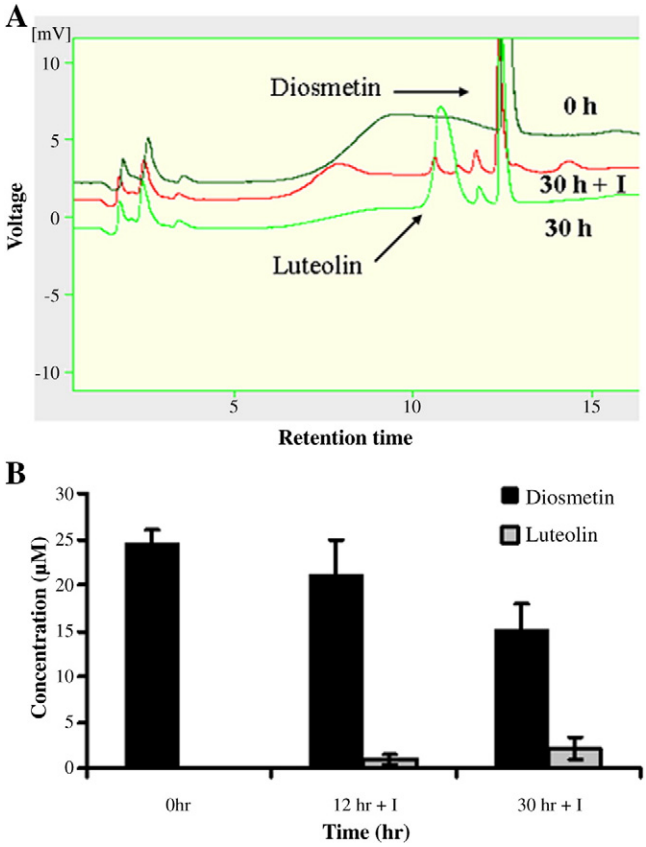

Fig. 3. The metabolism of diosmetin in HepG2 cells in the presence of the CYP1A inhibitor α-naphthoflavone. (A) HPLC trace of diosmetin (30 μM) incubation with HepG2 cells for 0- and 30-h time points in the presence (+I) or absence of the CYP1A inhibitor α-naphthoflavone. (B) Concentrations of diosmetin and luteolin after incubation with HepG2 cells for 0, 12 and 30 h in the presence (+I) of the CYP1A inhibitor α-naphthoflavone. Error bars indicate S.D. of the mean for $n=3$ experiments.

3.7. Diosmetin and luteolin induce up-regulation of the cell signaling proteins p-ERK, p-JNK, p53 and $p21^{CIP1/WAF1}$ in HepG2 cells

To further explore the mechanism of the antiproliferative action of diosmetin in HepG2 cells, the expression of cell signaling protein markers was investigated by Western blotting following treatment of the cells with diosmetin or luteolin for 24 h. Both diosmetin and luteolin increased the expression of the tumor suppressor protein p53 at comparable efficiencies at concentrations of 30 μM or higher (Fig. 7). In order to further investigate this finding, the expression of proteins that are active upstream in the cell signaling pathway, notably the two members of the MAPK kinase family, JNK and ERK, was investigated. The antibodies against JNK and its phosphorylated form identify total JNK expression which corresponds to JNK1 at 46 kDa and JNK2/3 at 54 kDa, whereas the antibody against the phosphorylated form of ERK is specific for both ERK1 and ERK2 at Thr/Tyr residues 202/204. Diosmetin induced up-regulation of p-JNK in a dose-dependent manner and of p-ERK at comparable potencies at concentrations of 30 μM or higher (Fig. 7). In contrast, luteolin did not seem to affect the levels of p-JNK, while it caused an increase of p-ERK at 30 and 50 μM and a decrease at 70 μM, as compared to β-actin control samples (Fig. 7). Neither diosmetin nor luteolin affected the expression levels of JNK, indicating that the effect on p-JNK seen with diosmetin occurs by phosphorylation and not by an increase in the total JNK levels (Fig. 7). In addition, diosmetin and luteolin did not affect expression of the cytoplasmic fraction of the transcription factor NFκB/p65 (Fig. 7) which is involved in cancer cell survival by triggering apoptosis invasion [27]. Our data further showed that p53 induction by both compounds resulted in up-regulation of $p21^{CIP1/WAF1}$, as the levels of this protein were markedly increased following treatment with diosmetin or luteolin (Fig. 7).

3.8. Induction of p53 and p-ERK by diosmetin is partially CYP1A mediated and reversible

The effect of diosmetin on p53 and p-ERK was investigated in the presence of the CYP1A inhibitor α-naphthoflavone. Diosmetin induced a strong up-regulation of p53 at the highest concentration when coincubated with α-naphthoflavone, whereas at the lower concentrations, the effect was rather weak and less than that of diosmetin alone (Figs. 7 and 8). Similarly, at a concentration of 30 μM of the compound in the presence of the inhibitor, the expression levels of p-ERK were comparable to the control sample containing 0.1% DMSO, and it was only at doses of 50 μM and higher that a modest increase was observed (Fig. 8).

4. Discussion

The metabolism of the natural flavonoid diosmetin in CYP1 (mainly CYP1A1) expressing human hepatoma cell line HepG2 was investigated. We report for the first time that in liver cancer cells diosmetin is converted to luteolin, which this coincides with growth arrest of the cells. More importantly, cell cycle arrest occurs as a result of the combined action of both diosmetin and luteolin and involves activation of the cell signaling proteins ERK, JNK and eventually p53 and p21 up-regulation.

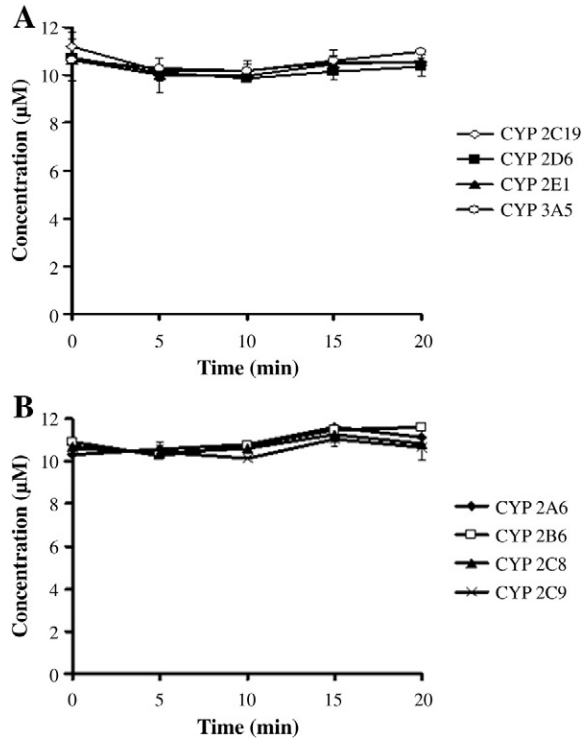

Fig. 4. The metabolism of diosmetin by a hepatic CYP panel. Diosmetin was incubated with recombinant CYP enzymes, and the concentration was estimated by HPLC as described in Materials and Methods. (A) Metabolism of diosmetin by recombinant CYP2C19, CYP2E1, CYP2D6 and CYP3A5. (B) Metabolism of diosmetin by recombinant CYP2A6, CYP2B6, CYP2C9 and CYP2C8. Error bars indicate S.D. of the mean for $n=3$ experiments.

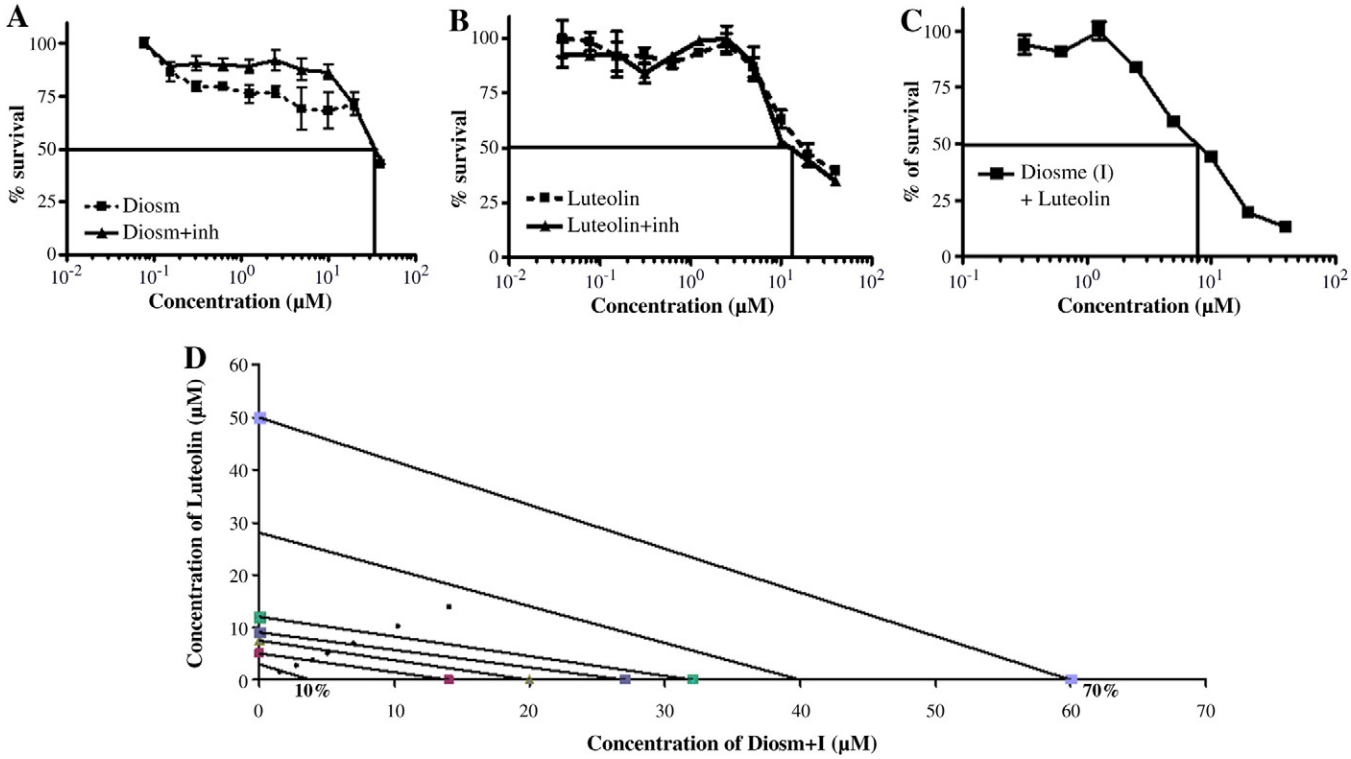

Fig. 5. The cytotoxicity of diosmetin (A), luteolin (B) and diosmetin with luteolin (C) in HepG2 cells. Flavonoids were incubated alone at a concentration range covering 0.078–40 μM for 96 h in the presence (+inh) or absence of the CYP1A inhibitor α-naphthoflavone, and cell viability was measured using the MTT assay as described in Materials and Methods. Diosmetin was added in the presence of the CYP1A inhibitor α-naphthoflavone (0.5 μM) at a concentration range of 40–0.3125 μM to HepG2 cells (C). Luteolin was added at the same concentrations with diosmetin in the absence of CYP1A inhibitor (C). Error bars indicate S.D. of the mean for $n=3$ experiments. (D) Isobologram analysis of diosmetin and luteolin.

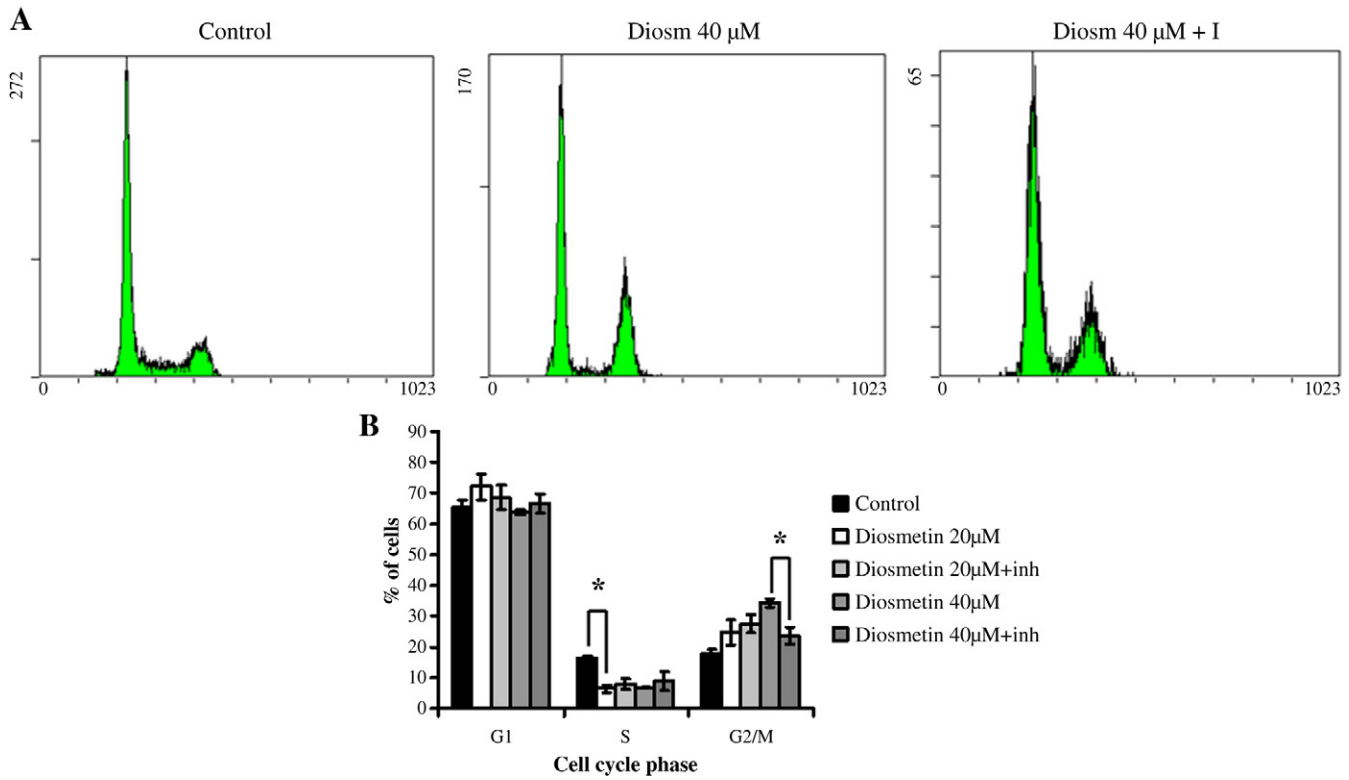

Fig. 6. Cell cycle profile of HepG2 cells following treatment with diosmetin (20 or 40 μM) for 24 h. The cells were treated with PI solution in PBS (50 μg/ml) containing RNase A (100 μg/ml), and fluorescence was measured using a Beckman Coulter flow cytometer as described in Materials and Methods. (A) Cell cycle histogram showing the results of 24-h incubation of the cells with 0.1% DMSO (control), 40 μM of diosmetin and 40 μM of diosmetin in the presence (+I) of 1 μM of α-naphthoflavone. (B) Percentage of HepG2 cells in each phase of the cell cycle measured following 20 or 40 μM of diosmetin treatment in the presence (+inh) or absence of 1 μM of α-naphthoflavone. Error bars are S.D. of the mean for at least $n=3$ determinations. *Statistically different ($P<.05$).

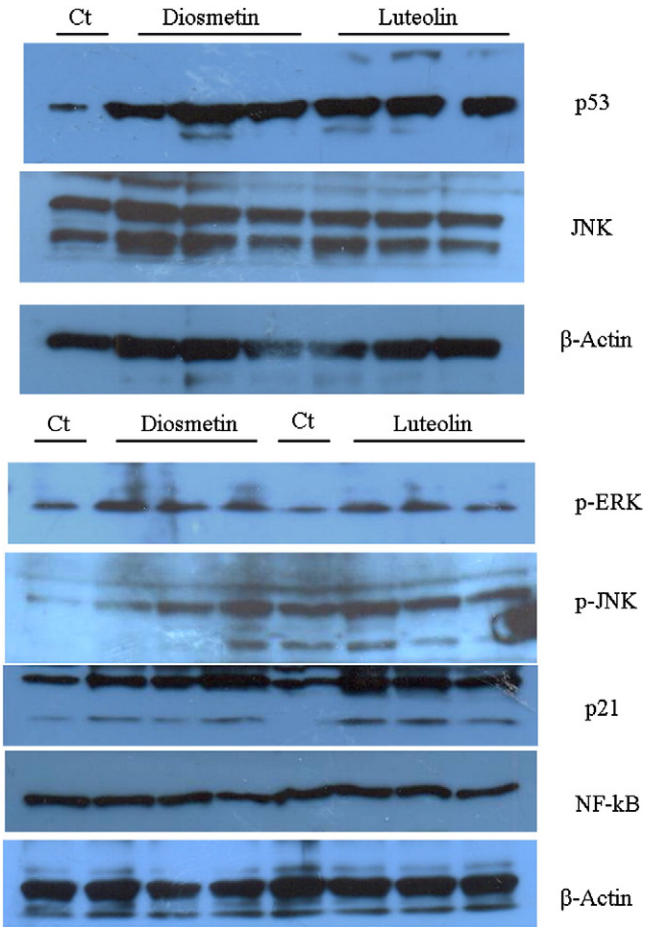

Fig. 7. Effects of diosmetin and luteolin on p53, JNK, p-JNK, p-ERK, p21 and NF-kB protein expression. β-actin was used as a loading control. HepG2 cells were treated with diosmetin or luteolin at concentrations of 30, 50 and 70 μM for 24 h, and Western blotting was carried out as described in Materials and Methods.

Expression of cytochrome P450 CYP1 enzymes in several cancer cell lines (MCF-7, LS180, Caco-2) has been evaluated previously [28,29]. HepG2 is a human liver cancer cell line that expresses CYP1 enzymes, as demonstrated by qPCR, EROD and B[a]P hydroxylase assays [22,23,30]. Given that CYP1A2 is a major liver phase-I enzyme, the finding that, in HepG2 cells, its expression was low compared to CYP1A1, as found in our and previous other studies, may initially seem paradoxical [22,23]. Although the expression of various metabolizing enzymes seems to be lower in HepG2 cells compared to human liver samples, CYP1A1 was found at equal or higher levels [22]. Ek and colleagues showed that CYP1A1 protein was expressed in HepG2 cells in the absence of any chemical inducers. However, this protein was not present in human hepatocytes [22]. The exact reason for this pattern of expression remains unclear, although a mechanism underlying posttranscriptional regulation on phase-I metabolizing enzymes involved in tumor progression may be possible [23,31]. It has been proposed that the decline in CYP1A2 expression in HepG2 cells reflects the possible "extinction" of the normal expression of the *CYP1A2* gene in this hepatoma-derived established cell line [23]. The higher levels of CYP1A1 expression in the tumor cell line HepG2 may indicate the implication of this enzyme in tumor progression by a mechanism poorly understood [31].

In HepG2 cells, diosmetin was metabolized to luteolin, as demonstrated by HPLC analysis. The formation of luteolin was evident at 12-h and peaked at 30-h treatment of diosmetin in HepG2 cells. The amount of metabolite formed at these time points probably relates to the levels of active CYP1 enzymes present in the cell line. Conversion of diosmetin into luteolin was previously demonstrated in recombinant CYP1 enzymes and in MCF-7 breast adenocarcinoma cells preinduced with dioxin [16]. The 4′-OCH_3 position of the B ring of flavonoids is an important structural feature that is essential for their substrate orientation to the active site of CYP1 enzymes [20,32]. Flavonoids that present similarities with respect to the structure of diosmetin have been shown to follow 4′-OCH_3 demethylations by CYP1 enzymes [21,33]. *In vitro* metabolism of hydroxylated flavonoids with vacant 4′ positions has further been shown to occur by previous studies from our group and others [34,35]. The results presented by such studies lead to the conclusion that the metabolite formed is usually more active in inhibiting proliferation of cancer cells than the parent compound [16,21,34,35]. The data presented herein seem at first glance to reinforce this finding, as luteolin, the metabolite of diosmetin, was more active in inhibiting proliferation of HepG2 cells in terms of IC50 values. However, when the simultaneous effects of diosmetin and luteolin were examined, the IC50 noted was considerably lower, whereas isobologram analysis revealed a synergistic mode of antiproliferative action. Synergistic interactions between structurally similar dietary flavonoids have been reported before in *in vitro* cancer cell lines [36].

Mechanistically, the antiproliferative effect of diosmetin was attributed to an arrest of the HepG2 cell cycle at the G2/M phase. This may in part be due to the cytotoxic effect of luteolin that has demonstrated DNA-topoisomerase I (Topo-I) inhibition [37]. Wang and coworkers showed in a recent study that diosmetin possesses some Topo-I inhibitory activity, but at a marginal level, in conjunction with low intercalation ability [38]. The planar structure of some flavonoids is an essential feature that contributes to partial DNA intercalating ability, while the methoxy group at position 4′ of diosmetin probably masks additional Topo-I inhibition compared to luteolin.

Induction of G2/M arrest by diosmetin was accompanied by a large accumulation of p53. In parallel, diosmetin induced p-ERK, whereas the metabolite luteolin caused a somewhat lesser induction of p-ERK at the highest concentration (70 μM). These findings may seem contradictory to the classical function of ERK which includes mitogenic stimulation and increased proliferative signals. However, during the last decade, increasing evidence has suggested that activated ERK is involved in activation of tumor suppressors such as p53. In the case of compounds such as doxorubicin that inhibit topoisomerase enzymes, the general concept suggests that induced stress or DNA damage activates ERK which in turn phosphorylates p53 at threonine residue 55 [39,40]. In the case of diosmetin or luteolin, p-ERK is possibly increased as a result of intracellular stress that further induces p53 and arrests the cells at G2/M. Consistent with

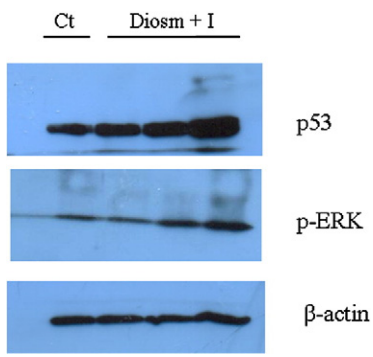

Fig. 8. Effects of diosmetin on p53 and p-ERK protein expression in the presence (+I) of α-naphthoflavone. HepG2 cells were treated with diosmetin at concentrations of 30, 50 and 70 μM and 1 μM of α-naphthoflavone for 24 h, and Western blotting was carried out as described in Materials and Methods.

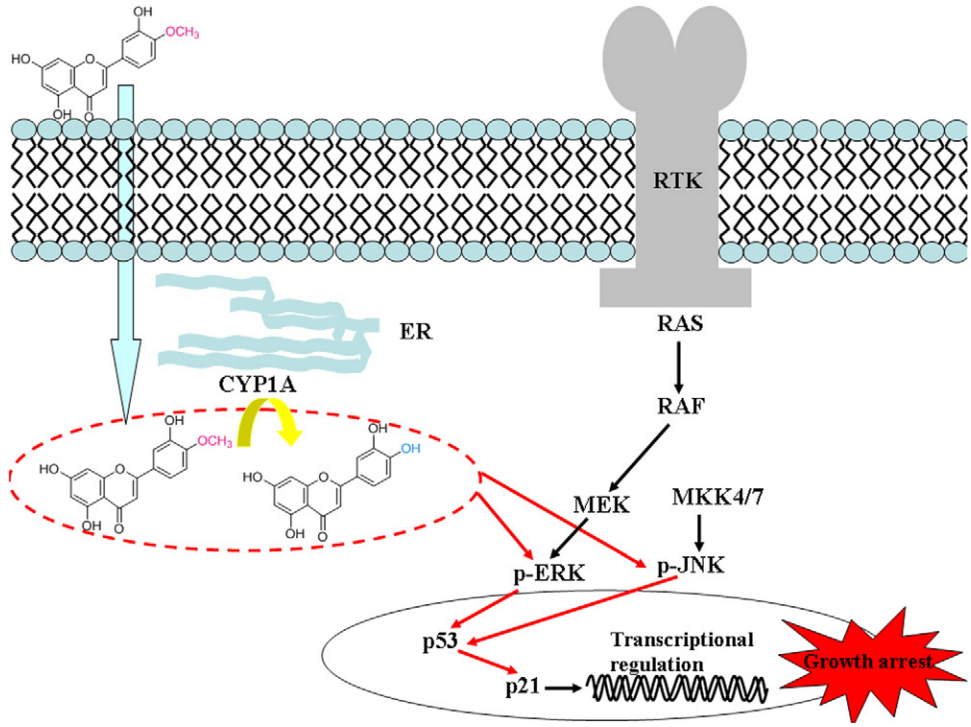

Fig. 9. Putative molecular pathway indicating the cell signaling events and metabolic effects mediated by diosmetin in liver cancer HepG2 cells.

this finding is the observation that, at very high concentrations (50 and 70 μM) of diosmetin or luteolin, p-ERK induction was attenuated, possibly as a result of early p53 induction. Importantly, this mechanism was CYP1A mediated since, in the presence of α-naphthoflavone, a much lesser induction of p53 and p-ERK was found. This scheme is outlined in Fig. 9.

The data further demonstrate that diosmetin induced increase of p-JNK in a dose-dependent way, whereas luteolin had little or no effect on the expression of this protein. In contrast, the expression levels of JNK remained relatively constant following treatment with diosmetin or luteolin, indicating that induction of p-JNK was due to activation of the protein and not due to an increase in the total JNK expression levels. Recent findings have shown that p-JNK physically interacts with p53 and stabilizes it by phosphorylation at residue threonine 81 [41]. JNK phosphorylation of p53 at threonine 81 is required for the dissociation of Ubc13 from p53, leading to p53 multimerization and transcriptional activation [41]. Decreased phosphorylation of p53 by p-JNK impairs its ability to induce growth arrest, growth inhibition and programmed cell death, all of which are responses to intracellular stress and DNA damage [42].

Expression levels of the transcription factor $p21^{CIP1/WAF1}$ increased following treatment of diosmetin or luteolin. $p21^{CIP1/WAF1}$ is a cell cycle inhibitor, involved primarily in the G1/S transition. $p21^{CIP1/WAF1}$ keeps retinoblastoma in its active hypophosphorylated state and arrests cells at the G1 phase ($p21^{CIP1}$). The second function of p21 is characterized as a gene activated by wild-type p53 ($p21^{WAF1}$). $p21^{WAF1}$ is essential in the regulation of the G2/M checkpoint by inhibiting cyclin-dependent kinase 1–cyclin B complex accumulation [43]. In the present study, we report that p53-mediated G2/M arrest of HepG2 cells by diosmetin is elicited via p21 up-regulation, possibly via conversion to the flavone luteolin. This is a phenomenon that has been observed previously in other cancer cell lines for structurally related flavonoids, notably luteolin, apigenin, chrysin, quercetin, kaempferol and myricetin [44].

With regard to the potential anticancer effects of diosmetin and luteolin *in vivo*, it is important to note that the concentration of dietary flavonoids in plasma varies according to parameters such as functional groups and daily intake. The concentration of the dihydroxylated flavonoid chrysin in plasma after a single dose of 400 mg has been estimated to be lower than 0.1 μM [45]. In contrast, methoxylated flavonoids exhibit up to 100-fold higher plasma concentrations due to reduced phase II conjugation reactions [45]. A recent study has underlined that the plasma concentration of flavonoids can increase significantly after daily supplementation for a prolonged period [46]. The polyhydroxylated flavonoid quercetin exhibited a plasma concentration of approximately 2–3 μM after 1000-mg daily dose for a period of 12 weeks [46]. Flavonoids with methoxy groups are expected to show higher plasma concentrations [45].

In conclusion, the present study investigated the anticancer effects of diosmetin and its metabolite luteolin in liver cancer HepG2 cells. The data demonstrate that diosmetin exerts a synergistic cytostatic action along with luteolin in order to arrest the cells at the G2/M phase. The mechanism of action involves activation of ERK and JNK by phosphorylation and subsequently p53 and p21 up-regulation. The results demonstrate that CYP1-activation of flavonoids may have therapeutic effects in tumors other than those derived from breast tissue.

Acknowledgments

We thank Eleni Koutala for excellent technical assistance of the flow cytometry expreriments and Dr Randolph Arroo for critical review of the manuscript.

References

[1] Poon RT, Borys N. Lyso-thermosensitive liposomal doxorubicin: an adjuvant to increase the cure rate of radiofrequency ablation in liver cancer. Future Oncol 2011;7:937–45.
[2] Kim NY, Sun JM, Kim YJ, Lee KW, Kim JH, Bang SM, et al. Cisplatin-based combination chemotherapy for advanced hepatocellular carcinoma: a single centre experience before the sorafenib era. Cancer Res Treat 2010;42:203–9.

[3] Yue OX, Liu X, Guo DA. Microtubule-binding natural products for cancer therapy. Planta Med 2010;76:1037–43.
[4] Wang LM, Ren DM. Flavopiridol, the first cyclin-dependent kinase inhibitor: recent advances in combination chemotherapy. Mini Rev Med Chem 2010;10: 1058–70.
[5] Mueller M, Lukas B, Novak J, Simoncini T, Genazzani AR, Jungbauer A. Oregano: a source for peroxisome proliferator-activated receptor gamma antagonists. J Agric Food Chem 2008;56:11621–30.
[6] Koukoulitsa C, Karioti A, Bergonzi MC, Pescitelli G, Di Bari L, Skalitsa H. Polar constituents from the aerial parts of *Origanum vulgare* L. Ssp. Hirtum growing wild in Greece. J Agric Food Chem 2006;54:5388–92.
[7] Doodstdar H, Burke MD, Mayer RT. Bioflavonoids: selective substrates and inhibitors for cytochrome P450 CYP1A and CYP1B1. Toxicology 2000;144:31–8.
[8] Xie YY, Yuan D, Yang JY, Wang LH, Wu CF. Cytotoxic activity of flavonoids from the flowers of *Chrysanthemum morifolium* on human colon cancer Colon205 cells. J Asian Nat Prod Res 2009;11:771–8.
[9] Bitis L, Kultur S, Melikoglu G, Ozsoy N, Can A. Flavonoids and antioxidant activity of *Rosa agrestis* leaves. Nat Prod Res 2010;24:580–9.
[10] AlGamdi N, Mullen W, Crozier A. Tea prepared from *Anstatica hirerochuntica* seeds contains a diversity of antioxidant flavonoids, chlorogenic acids and phenolic compounds. Phytochemistry 2011;72:248–54.
[11] Obmann A, Werner I, Presser A, Zehl M, Swoboda Z, Purevsuren S. Flavonoid C- and O-glycosides from the Mongolian medicinal plant *Dianthus versicolor* Fisch. Carbohydr Res 2011 in press.
[12] Pandino G, Courts FL, Lombardo S, Mauromicale G, Williamson G. Caffeoylquinic acids and flavonoids in the immature inflorescence of globe artichoke, wild cardoon and cultivated cardoon. J Agric Food Chem 2010;58:1026–31.
[13] Kato A, Minoshima Y, Yamamoto J, Adachi I, Watson AA, Nash RJ. Protective effects of dietary chamomile tea on diabetic complications. J Agric Food Chem 2008;56: 8206–11.
[14] Garcia-Gonzalez DL, Romero N, Aparicio R. Comparative study of virgin olive oil quality from single varieties cultivated in Chile and Spain. J Agric Food Chem 2010;58:12899–905.
[15] Seelinger G, Merfort I, Wolfle U, Schempp CM. Anti-carcinogenic effects of the flavonoid luteolin. Molecules 2008;13:2628–51.
[16] Androutsopoulos V, Arroo RR, Wilsher N, Potter GA. Bioactivation of the phytoestrogen diosmetin by CYP1 cytochromes P450. Cancer Lett 2009;274: 54–60.
[17] Patterson LH, Murray GI. Tumor cytochrome P450 and drug activation. Curr Pharm Des 2002;8:1335–47.
[18] Gribben JG, Ryan DP, Boyajian R, Urban RG, Hedley ML, Beach K, et al. Unexpected association between induction of immunity to the universal tumor antigen CYP1B1 and response to next therapy. Clin Cancer Res 2005;11:4430–6.
[19] Loaiza-Pérez AI, Kenney S, Boswell J, Hollingshead M, Alley MC, Hose C, et al. Aryl hydrocarbon receptor activation of an antitumour aminoflavone: basis of selective toxicity for MCF-7 breast tumour cells. Mol Cancer Ther 2004;3:715–25.
[20] Androutsopoulos VP, Papakyriakou A, Vourloumis D, Tsatsakis AM, Spandidos DA. Dietary flavonoids in cancer therapy and prevention: substrates and inhibitors of cytochrome P450 CYP1 enzymes. Pharmacol Ther 2010;126:9–20.
[21] Androutsopoulos V, Arroo RR, Hall JF, Surichan S, Potter GA. Antiproliferative and cytostatic effects of the natural product eupatorin on MDA-MB-468 human breast cancer cells due to CYP1 mediated metabolism. Breast Cancer Res 2008;10:R39.
[22] Ek M, Soderdahl T, Kuppers-Munther B, Edsbagge J, Anderson TB, Bjorquist P, et al. Expression of drug metabolizing enzymes in hepatocyte-like cells derived from human embryonic stem cells. Biochem Pharmacol 2007;74:496–503.
[23] Uno S, Endo K, Ishida Y, Tateno C, Makishima M, Yoshizato K, et al. CYP1A1 and CYP1A2 expression: comparing humanized mouse lines and wild-type mice; comparing human and mouse hepatoma cell lines. Toxicol Appl Pharmacol 2009;237:119–26.
[24] Burke MD, Mayer RT. Ethoxyresorufin: direct fluorimetric assay of a microsomal O-dealkylation which is preferentially inducible by 3-methylcholanthrene. Drug Metab Dispos 1974;2:583–8.
[25] Hewitt NJ, Hewitt P. Phase I and II enzyme characterization of two sources of HepG2 cell lines. Xenobiotica 2004;34:243–56.
[26] Boehme K, Dietz Y, Hewitt P, Mueller SO. Activation of p53 in HepG2 cells as surrogate to detect mutagens and promutagens in vitro. Toxicol Lett 2010;198: 272–81.
[27] Priyadarsini RV, Murugan RS, Maitreyi S, Ramalingam K, Karunagaran D, Nagini S. The flavonoid quercetin induces cell cycle arrest and mitochondria-mediated apoptosis in human cervical cancer (HeLa) cells through p53 induction and NF-kB inhibition. Eur J Pharmacol 2010;649:84–91.
[28] Beedanagari SR, Taylor RT, Bui P, Wang F, Nickerson DW, Hankinson O. Role of epigenetic mechanisms in differential regulation of the dioxin-inducible human CYP1A1 and CYP1B1 genes. Mol Pharmacol 2010;78:608–16.
[29] Netsch MI, Gutmann H, Schmidlin CB, Aydogan C, Drewe J. Induction of CYP1A by green tea extract in human intestinal cell lines. Planta Med 2006;72:514–20.
[30] Vrba J, Vrublova E, Modriansky M, Ulrichova J. Protropine and allocryptopine increase mRNA levels of cytochromes P450 1A in human hepatocytes and HepG2 cells independently of AhR. Toxicol Lett 2011;203:135–41.
[31] Androutsopoulos VP, Tsatsakis AM, Spandidos DA. Cytochrome P450 CYP1A1: wider roles in cancer progression and prevention. BMC Cancer 2009;9:187.
[32] Androutsopoulos VP, Papakyriakou A, Vourloumis D, Spandidos DA. Comparative CYP1A1 and CYP1B1 substrate and inhibitor profile of dietary flavonoids. Bioorg Med Chem 2011;19:2842–9.
[33] Cheng Z, Surichan S, Ruparelia K, Arroo RR, Boarder MR. Tangeretin and its metabolite 4′-hydroxytetramethoxyflavone attenuate EGF-stimulated cell cycle progression in hepatocytes; role of inhibition at the level of mTOR/p70S6K. Brit J Pharmacol 2011;162:1781–91.
[34] Atherton KM, Mutch E, Ford D. Metabolism of the soyabean isoflavone daidzein by CYP1A2 and the extra-hepatic CYPs 1A1 and 1B1 affects biological activity. Biochem Pharmacol 2006;72:624–31.
[35] Androutsopoulos VP, Ruparelia K, Arroo RR, Tsatsakis AM, Spandidos DA. CYP1-mediated antiproliferative activity of dietary flavonoids in MDA-MB-468 breast cancer cells. Toxicology 2009;264:162–70.
[36] Zhang S, Yang X, Morris ME. Combined effects of multiple flavonoids on breast cancer resistance protein (ABCG2)-mediated transport. Pharm Res 2004;21: 1263–73.
[37] Galvez M, Martin-Cordero C, Lopez-Lazaro M, Cortes F, Ayuso MJ. Cytotoxic effect of *Plantago* spp. on cancer cell lines. J Ethnopharmacol 2003;88:125–30.
[38] Wang P, Li S, Ownby S, Zhang Z, Yuan W, Zhang W. Ecdysteroids and a sucrose phenylpropanoid ester from *Froelichia floridana*. Phytochemistry 2009;70:430–6.
[39] Yeh PY, Chuang SE, Yeh KH, Song YC, Chang LLY, Cheng AL. Phosphorylation of p53 on Thr55 by ERK2 is necessary for doxorubicin-induced p53 activation and cell death. Oncogene 2004;23:3580–8.
[40] Singh S, Upadhyay AK, Ajay AK, Bhat MK. p53 regulates ERK activation in carboplatin induced apoptosis in cervical carcinoma: a novel target of p53 in apoptosis. FEBS Lett 2007;581:289–95.
[41] Topisirovic I, Gutierrez GJ, Chen M, Appella E, Borden KL, Ronai ZA. Control of p53 multimerisation by Ubc13 is JNK-regulated. Proc Natl Acad Sci USA 2009;106: 12676–81.
[42] Buschmann T, Potapova O, Bar-Shira A, Ivanov VN, Fuchs SY, Henderson S, et al. Jun NH2-terminal kinase phosphorylation of p53 on Thr-81 is important for p53 stabilization and transcriptional activities in response to stress. Mol Cell Biol 2001;21:2743–54.
[43] Huang HS, Liu ZM, Ding L, Chang WC, Hsu PY, Wang SH, et al. Opposite effect of ERK1/2 and JNK on p53-independent $p21^{WAF1/CIP1}$ activation involved in the arsenic trioxide-induced human epidermoid carcinoma A431 cellular cytotoxicity. J Biomed Sci 2006;13:113–25.
[44] Zhang Q, Zhao XH, Wang ZI. Cytotoxicity of flavones and flavonols to a human esophageal squamus cell carcinoma cell line (KYSE-510) by induction of G2/M arrest and apoptosis. Toxicol In Vitro 2009;23:797–807.
[45] Walle T. Methylation of dietary flavonoids greatly improves their hepatic metabolic stability and intestinal absorption. Mol Pharmaceutics 2007;6: 826–32.
[46] Heinz SA, Henson DA, Nieman DC, Austin MD, Jin F. A 12-week supplementation with quercetin does not affect natural killer cell activity, granulocyte oxidative burst activity or granulocyte phagocytosis in female human subjects. Br J Nutr 2010;104:849–57.